A theoretical study of the isotropic cut sphere fluids

Antoine Chamoux and Aurélien Perera

Citation: The Journal of Chemical Physics **108**, 8172 (1998); doi: 10.1063/1.476172
View online: http://dx.doi.org/10.1063/1.476172
View Table of Contents: http://scitation.aip.org/content/aip/journal/jcp/108/19?ver=pdfcov
Published by the AIP Publishing

A theoretical study of the isotropic cut sphere fluids

Antoine Chamoux and Aurélien Perera
Laboratoire de Physique Théorique des Liquides, Université Pierre et Marie Curie, 4, place Jussieu, 75252 Paris Cedex 05, France

(Received 3 November 1997; accepted 11 February 1998)

The cut sphere fluid is studied in the isotropic phase by the Percus Yevick (PY) and the Hypernetted Chain (HNC) integral equation techniques, as well as by the theory recently proposed which is based on a geometrical interpretation of the direct correlation function. Fluids of cut spheres with thicknesses L^* ranging from 0 to 0.7 have been studied, and detailed results for $L^*=0.1$, 0.2, and 0.3 are reported. The $L^*=0$ case is also examined. A new simplified version of the numerical implementation of the PY and HNC closures is proposed here. The results for pressures and structural properties are compared with the available simulations results and the recent theoretical results from the authors. The important feature of the present work is to show the ability of the HNC theory to predict the *cubatic* phase observed in the computer simulations for thicknesses around 0.2. The nematic phase is also predicted by the HNC theory for thicknesses smaller than $L^*=0.12$. In agreement with previously obtained results, the detailed analysis of the PY theory results show that this approximation is unable to predict an instability toward any of the orientationally ordered fluid phases. The geometrical approach shows the correct trend for an isotropic to nematic transition, but exhibits an instability toward the *cubatic* phase only for thicknesses above $L^*=0.5$, thus providing an illustration of the inability of standard density functional type theories to fully describe complex fluids. This study also sheds some light on the major differences between the three approaches in the treatment of many body density correlations. © *1998 American Institute of Physics.* [S0021-9606(98)51419-5]

I. INTRODUCTION

Real mesogens have rich phase diagrams, and lyotropic liquid crystals, in particular, can have various type of ordered phases, including micellar phases.[1] They are particularly interesting from a modeling point of view as one can use hard core models such as hard convex bodies. There is still a long way to go from these crude models to real lyotropic molecules, but this modeling is adequate in the sense that it can capture the essential liquid ordering features. Computer simulations have played a major role in the understanding of these model fluids, and a beautiful example is the recent calculation of the global phase diagram for prolate sphero-cylinders.[2] Fluids of cut spheres stand apart from the rest of the models as they exhibit, in addition to the nematic, columnar, and solid phases, a novel liquid phase characterized by a *cubatic* order. This was put into evidence by Veerman and Frenkel using computer simulations.[3,4] This cubatic order is characterized by perpendicular alignment of short stacks of cut spheres, and this order is long range. To our knowledge, no theoretical approaches have been used to show this particular feature of the cut sphere fluid.

Density functional theories have been the most successful in describing mesogenic phase transformations such as isotropic-nematic-smectic. The major ingredient of such theories is the direct correlation function (DCF) usually approximated (with various level of sophistication) essentially by the Mayer function which involves the pair interaction only. Although such an approach seems sufficient for describing nematic or smectic type ordering, it remains unclear as to whether it can provide a correct description of the cubatic ordering. Integral equations methods, mainly the Percus Yevick (PY) and Hypernetted Chain (HNC) theories, have been shown to adequately describe the structure and the thermodynamics of several nonspherical hard core fluids in their isotropic phase.[5] However, their accuracy is mostly limited to low to medium densities and their ability to describe *fluctuating* ordered phases remains still unanswered. The HNC theory in particular does account for the orientational instability of the isotropic phase and thus provides an indirect guess of the next ordered phase. The integral equations have been used to study the *rigidly* aligned cut sphere fluids and evidence for columnar ordering was found.[6]

The aim of the present work is twofold. First, the ability of the integral equations to predict the isotropic-nematic (IN) instability as well as the isotropic-cubatic instability is tested. A new, simplified solution method for solving the integral equations is proposed here, which allows in particular getting closer to the instability region of the isotropic phase. From previous works it was found that the PY theory was inadequate to describe the nematic pretransitional ordering. It is not obvious to conclude that this theory will also fail for the case of the cubatic pretransitional ordering. Second, the DCFs obtained by solving the integral equations provide a good test of the recently proposed geometrical approach for the DCF of convex fluids, mainly in the low to moderately high density region where the integral equations are supposed to work well. Results from both approaches can be then compared with the computer simulations.[4]

This paper is organized as follows. The next section is a

brief remainder of the integral equation methods, mainly concerning the new solution technique, as well as the geometrical approach mentioned above. The detailed results of the thermodynamics and the structural features of the cut spheres are presented in Sec. III. Finally, Sec. IV presents our conclusions about the three methods presented herein.

II. THEORY

The integral equations techniques for nonspherical particles are now well known and commonly used by numerous authors. Hence, only the major material needed to understand the context will be displayed in the next subsections.

A. Integral equations

Essentially two methods have been proposed in the current literature to solve the PY or HNC integral equations together with the Ornstein-Zernike (OZ). They differ in the way in which the closures are treated. The pair and direct correlation functions are usually expanded in a basis of rotational invariants describing the symmetry of the phase under study, which allows a nice decoupling between the radial and angular variables. For the isotropic phase of fluids of uniaxial particles such expansion for the pair distribution function reads.[7]

$$g(1,2)=\sum_{mnl} g^{mnl}(r)\Phi^{mnl}(\mathbf{\Omega}_1,\mathbf{\Omega}_1,\hat{\mathbf{r}}), \tag{1}$$

where (1,2) stands for $(\mathbf{r}_{12},\ \mathbf{\Omega}_1,\ \mathbf{\Omega}_2)$, $\mathbf{r}_{12}$ is the intermolecular vector, and $\mathbf{\Omega}_i$ is the Euler angle describing the orientation of the ith particle. The rotational invariant $\Phi^{mnl}(1,2)$ only depends on the three Euler angles and is explicited in Ref. 7. Similar expansion also holds for the direct correlation function $c(1,2)$. The OZ equation is solved identically by both methods and solely involves the expansion coefficients and their Fourier-Hankel transforms. The HNC closure involves an exponentiation $g(1,2)=\exp(-\phi(1,2)+\eta(1,2))$, where $\phi(1,2)$ is the intermolecular potential and $\eta(1,2)=g(1,2)-1-c(1,2)$. The method originally proposed by Lado[8] consists of expanding the exponential by computing the exponent as a function depending on *all* the radial and angular variables. This involves first a reconstitution of the exponent using Eq. (1) and then an expansion for $g(1,2)$ in order to get the expansion coefficients $g^{mnl}(r)$, and this must be done at every stage of the iterative solution procedure. The other method proposed by Fries and Patey[9] involves only the expansion coefficients and expresses the HNC closure in a integro-differential form. We will use the second method because it is numerically simpler. This latter method was previously used[5] to solve the integral equation for various nonspherical particles. It had the inconvenience of the heavy computation of a large number of overlap coefficients $A^{mnl}_{m_1n_1l_1}(r)$. The solution of the same closure for the two dimensional system[10] was surprisingly simpler as in this case the overlap coefficients were identical to the expansion coefficients of the Mayer function. We show here that a unified form of the closure can also be proposed, which makes it valid for all dimensions.

For nonspherical hard core fluids the general closure form can be written as

$$c(1,2)=-F_M(1,2)c_{OV}(1,2)+(1+F_M(1,2))c_{NOV}(1,2) \tag{2}$$

in terms of the Mayer function $F_M(1,2)=\exp(-\phi(1,2))-1$. $c_{ov}(1,2)$ is the closure relation for direct correlation function in the overlap domain of the two particles [resp. $c_{NOV}(1,2)$ for the nonoverlapping domain]. This equation simply expresses the fact that $F_M(1,2)=-1$ in the overlap domain and $F_M(1,2)=-0$ outside this domain. The closure is completed by the specification of the expressions for c_{ov} and c_{NOV}:

$$c_{OV}(1,2)=-1-\eta(1,2). \tag{3}$$

This equation exactly expresses that $g(1,2)=0$ in the hard core overlap region. The PY closure for hard cores is

$$c_{NOV}(12)=0 \tag{4}$$

and the HNC closure is[9]

$$c_{NOV}(12)=\int_0^\infty dr'\ \frac{d\eta(1,2)}{dr'}\ (g(1,2)-1). \tag{5}$$

Expanding Eq. (2) one gets

$$c^{mnl}(r)=c^{mnl}_{NOV}(r)+\sum_{m_1n_1l_1}\sum_{m_2n_2l_2} PF_M^{m_1n_1l_1}(r) \times(c_{NOV}^{m_2n_2l_2}(r)-c_{OV}^{m_2n_2l_2}(r)), \tag{6}$$

where the coefficient P, which depends on all the nine indices, appears in the expansion of the product of two invariants:[9] $\Phi^{m_1n_1l_1}\Phi^{m_2n_2l_2}=\Sigma_{mnl}P\Phi^{mnl}$. It is easy to show[11] that the overlap coefficients used in Ref. 5 are related to the expansion coefficients $F_M^{mnl}(r)$. In particular one has

$$A^{mnl}_{000}(r)=-I^{mnl}F_M^{mnl}(r), \tag{7}$$

where $I^{mnl}=\int d1\,d2[\Phi^{mnl}(1,2)]^2$ is the normalization of the rotational invariants. This relation shows the dramatic decrease in complexity which is involved in the new formulation of the closure, as the number of overlap coefficients varies like the square of the number of expansion terms retained in Eq. (1). The basic advantage of the new method (in addition to saving storage space and CPU time) is that the integral equation can be solved for somewhat higher densities than was previously possible. This allows getting closer to the limit of the instability of the isotropic phase and consequently having a better guess of the type of the ordered phase to which it leads to. These points are detailed in Sec. III.

B. The geometrical DCF

In Ref. 12 we have put forward a new approximation for the direct correlation function of convex molecular shapes, which was based on the geometrical properties of single particles. This approximation was formulated for the general case of mixtures and was shown to be quite accurate for various convex shapes. We briefly recall here the major results of the geometrical approach. In this approach the DCF is approximated by

$$c(1,2) = -\chi_V \Delta V(1,2) - \chi_S \Delta S(1,2) + \chi_0 F_M(1,2), \quad (8)$$

where $\Delta V(1,2)$ is the overlap volume of particles 1 and 2, and $\Delta S(1,2)$ is the corresponding overlap surface. The density dependent coefficients χ_a are functions of the generalized scaled particle (SPT) variables $\eta_\alpha = \rho R_\alpha$ defined as functions of the density ρ and the geometrical characteristics of the individual convex particle which are the volume $R_3 = V$, the surface $R_2 = S$, the mean radius $R_1 = R_m$, and finally $R_0 = 1$. The corresponding definitions for mixtures are also given in Ref. 12. The χ_a coefficients are related to the second derivatives of the excess free energy with respect to the η_α and the form of the free energy was taken from compressibility SPT form:[13]

$$\Phi^{(C)} = -\eta_0 \ln(1-\eta_3) + \frac{\eta_1 \eta_2}{1-\eta_3} + \frac{1}{24\pi} \frac{\eta_2^3}{(1-\eta_3)^2}, \quad (9)$$

and the χ_a are explicitly defined as

$$\chi_V = \Phi_{33}^{(C)},$$

$$\chi_S = \Phi_{32}^{(C)} + \Phi_{31}^{(C)} \frac{\gamma}{8\pi},$$

$$\chi_0 = \Phi_{30}^{(C)} + \Phi_{31}^{(C)} \frac{R_m^2 \gamma}{2}, \quad (10)$$

where $\gamma = (2R_m V + S^2/(4\pi))/(SV/(4\pi) + R_m^2 B_2)$ and B_2 is the second virial coefficient known analytically for convex bodies. We have used the following notation for the second derivatives: $\Phi_{\alpha\beta}^{(C)} = \partial^2 \Phi^{(C)} / \partial \eta_\alpha \partial \eta_\beta$.

In the hard sphere limit, the DCF thus constructed reduces exactly to the PY solution. The nice separation in Eq. (8) between the density dependent coefficients and the geometrical function makes this approximation quite appealing. In the original derivation for the hard sphere case[14,15] the DCF was expressed entirely in terms of convolution of weight functions specific of the geometrical properties of individual hard sphere components. However, this nice feature was shown to be inadequate for the general case of convex bodies when applied as such.[12] In particular, a straightforward extension of the PY hard sphere DCF to convex bodies does not lead to the true PY results as obtained numerically. Moreover, this DCF was shown to be isotropic in the limit $k = 0$, a feature which is again not shared by the true PY solution. The major consequence is that, unlike hard spheres, the Mayer function of convex bodies in general cannot be represented as a convolution of weight functions. This function was thus properly introduced, leading to several possibilities for new approximate DCF among which the expression in Eq. (8) was found to closely fit the true PY DCF. The major drawback of these new approximations is that the corresponding pair distribution functions are nonzero inside the hard core overlap region.

Unlike the Mayer function, the overlap volume and surface can generally be represented as convolution of weight functions

$$\Delta V(1,2) = w^{(3)}(1) * w^{(3)}(2),$$

$$\Delta S(1,2) = w^{(3)}(1) * w^{(2)}(2) + w^{(3)}(2) * w^{(2)}(1), \quad (11)$$

where $*$ denotes a convolution product over the separation variable $\mathbf{r}$. The volume and surface weight functions [$w^{(3)}(1)$ and $w^{(2)}(1)$, respectively] depend only in the single particle position $\mathbf{r}$ and orientation described by the Euler angle $\mathbf{\Omega}$ $w^{(\alpha)}(1) = w^{(\alpha)}(\mathbf{r}, \mathbf{\Omega})$. They are explicitly defined in Ref. 12 and are listed therein for several convex bodies including the cut spheres. Some preliminary results for cut spheres are also mentioned in this reference.

The equation of state (EOS) can be derived by the compressibility route from Eq. (8), by the standard thermodynamic integration $\beta P/\rho = 1 - (1/\rho) \int_0^\rho d\rho' \tilde{c}^{000}(0)$ where $\tilde{c}^{000}(0)$ is the $k = 0$ limit of the Fourier-Hankel transform of $c^{000}(r)$. The form of Eq. (8) guarantees that the EOS thus obtained is consistent with the form of the free energy that is chosen to derive the χ_a coefficients. As a consequence, the compressibility pressure is that of the SPT theory and is given by[13]

$$\beta P_C = \frac{\eta_0}{1-\eta_3} + \frac{\eta_1 \eta_2}{(1-\eta_3)^2} + \frac{1}{12\pi} \frac{\eta_2^3}{(1-\eta_3)^3}. \quad (12)$$

However, the SPT virial pressure[13]

$$\beta P_V = \frac{\eta_0}{1-\eta_3} + \frac{\eta_1 \eta_2}{(1-\eta_3)^2} + \frac{1}{12\pi} \frac{\eta_2^3}{(1-\eta_3)^2} \quad (13)$$

is not given by the geometrical DCF approach, a feature which is again a consequence of the mathematical impossibility of expressing DCF of convex bodies as a convolution of weights. In addition, it was found in Ref. 12 that the SPT virial and compressibility pressure were again different from that obtained from the numerical PY solution, thus confirming the inability of the spherical SPT weighted density functional theory[14,15] to be extended to convex bodies.

The great advantage of Eq. (8) is then to have an analytical compressibility pressure as well as to reproduce very well the general features of the DCF of convex bodies when compared with the HNC and PY results. Another nice feature is that the Carnahan-Starling (CS) type EOS formed from the SPT pressures ($P = (2P_C + P_V)/3$) is surprisingly accurate for prolate anisotropic convex bodies (up to aspect ratio of 5), and particularly, the virial coefficients that can be extracted from this equation also be quite accurate up to fifth order.[12]

We finally note that this approximation has been recently successfully extended to nonconvex bodies such as tangent and fused hard sphere chains.[16,11]

III. RESULTS

The ingredient common to both the solution of the integral equations and the geometrical DCF is the Mayer function, and more particularly the expansion coefficients $F_M^{mnl}(r)$. Using Eq. (8) one can basically compute such coefficients using an algorithm sketched in Ref. 5. An improved algorithm have been proposed recently[11,16] which reduces the number of angular integrations, allowing thus for a better accuracy. The calculation of the $F_M^{mnl}(r)$ rests on a precise determination of the contact distances between two particles. For the case of cut spheres this calculation is quite involved.[11] The calculated expansion coefficients are found

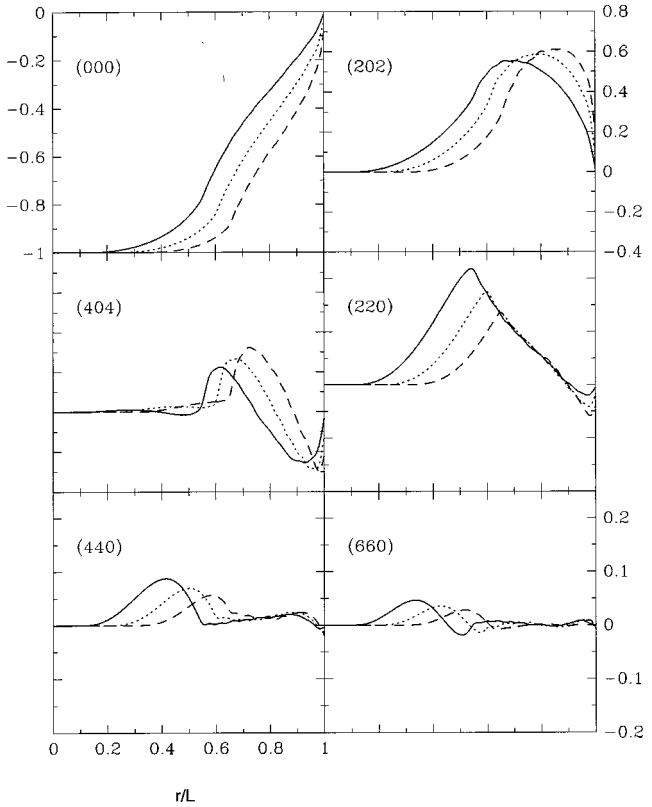

FIG. 1. The Mayer function expansion coefficients $F_M^{mnl}(r)$ for cut spheres of thicknesses $L^*=0.1$, 0.2, and 0.3. The upper right vertical scale is for both $(m0m)$ terms and the lower right scale is for all the $(mm0)$. The projections indices are indicated in parenthesis. The solid line is for $L^*=0.1$, the dotted line for $L^*=0.2$, and dashed line for $L^*=0.3$.

to be relatively smooth oscillatory functions of the distance r. The accuracy of their calculation can be tested by numerically determining the second virial coefficient from $B_2=-\tilde{F}_M^{000}(k=0)/2$ and comparing it to the exact value known analytically for convex bodies $B_2=V+SR_m$. In all cases, even for very anisotropic shapes, the agreement is better than one percent.[17] The equivalent test for higher order coefficients can be obtained when the $B_2(\gamma)$ is known analytically (γ is the angle between the molecular axis of the two particles). In such a case one can compare all $\tilde{F}_M^{mm0}(k=0)$ with the Legendre polynomial expansion of $B_2(\gamma)$. For convex bodies this is possible only for sphero cylinders[18] and infinitely thin platelets.[19] In the latter case one has exactly $\tilde{F}_M(k=0,\ \cos\gamma=\mathbf{u}_1\cdot\mathbf{u}_2)=-(\pi/2)|\sin\gamma|$ where $\mathbf{u}_i$ is a unit vector along the molecular axis of cut sphere i. Among nonconvex shapes, the tangent hard spheres chains and the Gaussian overlap model also allow this calculation. In such cases, the test gives accurate values of up to $m=8$ (less than five percent at most[17]). This is more than sufficient for our purpose, as in practice the expansion in Eq. (1) is carried only up to the order $m_{\max}=6$. For the cut sphere case, as mentioned above, only F_M^{000} can be tested. Some of the $F_M^{mnl}(r)$ are plotted in Fig. 1 for a cut sphere thickness of $L^*=L/\sigma=0.1$, 0.2, and 0.3, where σ is the diameter of the hard sphere. The computer simulation results[4] have been reported for precisely these thickness values. We note that these functions are discontinuous at $r^*=r/L=1$ because of the rolling contact that occurs between the spherical parts of the two cut spheres. This discontinuity is also present in the correlation functions and must be handled properly during the solution procedure.[11] Small oscillations are present for distances just below $r^*=1$ in the region of contacts between the edges of one cut sphere with either the plane or the spherical part of the second cut sphere. These oscillations are numerical inaccuracies due to the difficulty of describing by a finite number of invariants the abrupt orientational changes that occur in this region when two cut spheres are displaced relatively to each other. These oscillations persist even with finer angular grid width are used to perform the integrations. They do not appear for other convex shapes which have smoother shapes. These oscillations do not affect, however, the accuracy of the calculated second virial coefficients.

Table I shows some of the Mayer function expansion coefficients $\tilde{F}_M^{mm0}(k=0)$ for several thicknesses. First of all we see that there is a remarkable agreement for the $L^*=0$ case, between the exact results and those obtained by integrating the $F_M^{mm0}(r)$. The same agreement also holds for nonzero thicknesses. The second feature is that the values for $\tilde{F}_M^{440}(0)$ *increase* with decreasing values of thicknesses until approximately $L^*\geqslant 0.3$, and they become *larger* than the values of $\tilde{F}_M^{220}(0)$ for thicknesses above $L^*=0.43$. Similarly, the values of $\tilde{F}_M^{660}(0)$ also become larger than $\tilde{F}_M^{220}(0)$ around $L^*=0.6$. The usual rule for several other convex and nonconvex bodies is that all the $\tilde{F}_M^{mm0}(0)$ are decreasing functions of m and aspect ratios. So the cut spheres represent a curious exception. As the Mayer function represents exactly all the two body interactions, the behavior of $\tilde{F}_M^{440}(0)$ is certainly the signature of the possibility of a cubatic order-

TABLE I. Comparison between the exact and numerically evaluated (respectively upper and lower line values) Mayer function expansion coefficients $\tilde{F}^{mm0}(k=0)$ for cut spheres of thicknesses L^*.

L^*	0	0.1	0.2	0.3	0.4	0.5	0.7	1
$m=0$	−1.2337	−1.7111	−2.1704	−2.6010	−2.9938	−3.3409	−3.8722	−4.1888
	−1.2381	−1.7086	−2.1686	−2.5984	−2.9902	−3.3278	−3.8770	
$m=2$	0.3443	-	-	-	-	-	-	0
	0.3448	0.2666	0.1953	0.1334	0.0814	0.0492	0.00614	
$m=4$	0.0572	-	-	-	-	-	-	0
	0.0578	0.0724	0.0806	0.0823	0.0740	0.0583	0.01854	
$m=6$	0.0217	-	-	-	-	-	-	0
	0.0222	0.0160	0.0137	0.0115	0.0127	0.0149	0.01241	

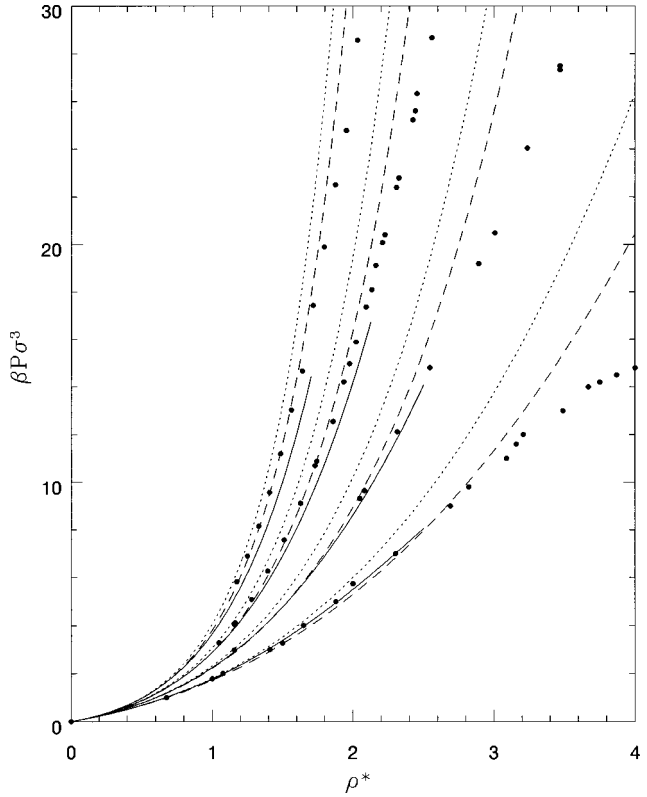

FIG. 2. The equation of state for cut spheres of thicknesses $L^*=0.0.1$, 0.2, and 0.3. The solid line is for HNC(C), the dotted line for PY(C), and dashes for SPT Carnahan-Starling expression (see text). The dots are simulations results from Refs. 20 and 4. The thicknesses are, starting from the topmost set of curves, $L^*=0.3$, 0.2, 0.1, and $L^*=0$.

ing. We return to this point in the subsection on the instability of the isotropic phase.

In the following section we present our results for the same values as the simulations, including $L^*=0$, which correspond to a platelet shape for which Frenkel has also reported simulation results.[20] We used density units $\rho^*=\rho\sigma^3$.

A. Results for the pressures

The compressibility pressures as obtained from the integral equations and the SPT-C expression Eq. (12) are plotted in Fig. 2 together with the Carnahan-Starling and the computer simulation results. For large L^* values, in particular here $L^*=0.3$, the pressures from the integral equations bracket the computer simulation results, a situation which is quite similar to the hard sphere case. The CS pressures do not fit the computer simulation results in the same wide range as they do in the hard sphere case. As the thickness is increased, the situation gets closer to that of the hard sphere limit, as one can expect. For the case $L^*=0.2$ we see that globally the HNC compressibility pressure is in closer agreement with the simulation results. This trend even increases with $L^*=0$ and 0.1 for which the agreement between HNC and the simulations is near perfect. However, it is clear that as L^* decreases, the density range over which HNC can be solved decreases dramatically as compared with that of the PY theory. This is related to the range of stability of the isotropic phase which is smaller for HNC than for PY. We note that the SPT approach gets worse for more oblate shapes. A similar trend was found in Ref. 12 with oblate ellipsoids. We also note that, as L^* gets smaller, the computer simulation pressures become increasingly flattened. For the case $L^*=0$ it was found[20] that some higher virial coefficients were negative, leading to the flattening observed in the pressure curve. The geometrical approach, on the other hand, predicts that all order virial coefficients are positive, thus the curvature of the SPT pressure is always steeper. Results for PY also have a similar behavior. On the other hand, the HNC theory which predicts exact fourth order virial coefficient seems to follow the correct trend, and it might be that the HNC fifth order virial coefficient can be negative. It is, however, very difficult to confirm this numerically as the polynomial fit is very noisy, mainly as higher order terms become very small. We see that for $L^*=0$ the CS pressure is too low at small densities, a feature that is absent from PY and HNC results. This can be explained by the fact that the CS EOS contains only the correct second virial coefficient whereas PY and HNC contain correct higher order ones. As all the virial coefficients of the CS EOS are positive, one can expect from the high density behavior that some of the higher virial coefficients from HNC could be negative.

B. Results for the correlation functions

In Fig. 3(a) we compare various expansion coefficients of the pair distribution function $g^{mnl}(r)$ between the PY and the HNC theories, for cut sphere thickness $L^*=0.3$ and for the density $\rho^*=1.7037$. This is the highest density for which the HNC theory could be solved in this case. The global features are similar to those observed in Fig. 1 [which correspond in fact to the case $\rho^*=0$ where $g_{\rho=0}(1,2)=1+F_M(1,2)$], but they have more prominent structures, and the structure is different for both theories. As the same trends are also observed for smaller thicknesses it is worth analyzing this case thoroughly. Both theories show a discontinuity at $r^*=1$, which correspond to the rolling contact between the spherical parts of the two cut spheres. From examining $g^{000}(r)$ for smaller r^*, we see that HNC predicts a three particles piling in a short column, whereas PY predicts a loose structure peaked around $r^*=0.75$ which corresponds in fact to a loose perpendicular alignment. The presence of HNC of the smaller peak near $r^*=0.45$ indicates this tendency of a stack piling (perfect piling would be for $r^*=0.3$) and this feature is completely absent from PY. We also note that the second peak for HNC is at a smaller distance than the first PY peak, thus confirming the tendency to stack piling. The orientational components $g^{220}(r)$ and $g^{440}(r)$, and to some extent $g^{202}(r)$, again confirm these tendencies. In particular, the negative well of $g^{220}(r)$ around $r^*\sim 0.7$ precisely corresponds to a perpendicular particles configuration. The computer simulation reports only two phases for this system, an isotropic liquid and a solid phase. Although there seems to be a tendency to cubatic ordering, this phase turns out to be metastable. From what we have observed we can say that the HNC theory supports a tendency toward cubatic phase. However, analysis of the stability shows that cubatic phase is ruled out, in accord with the

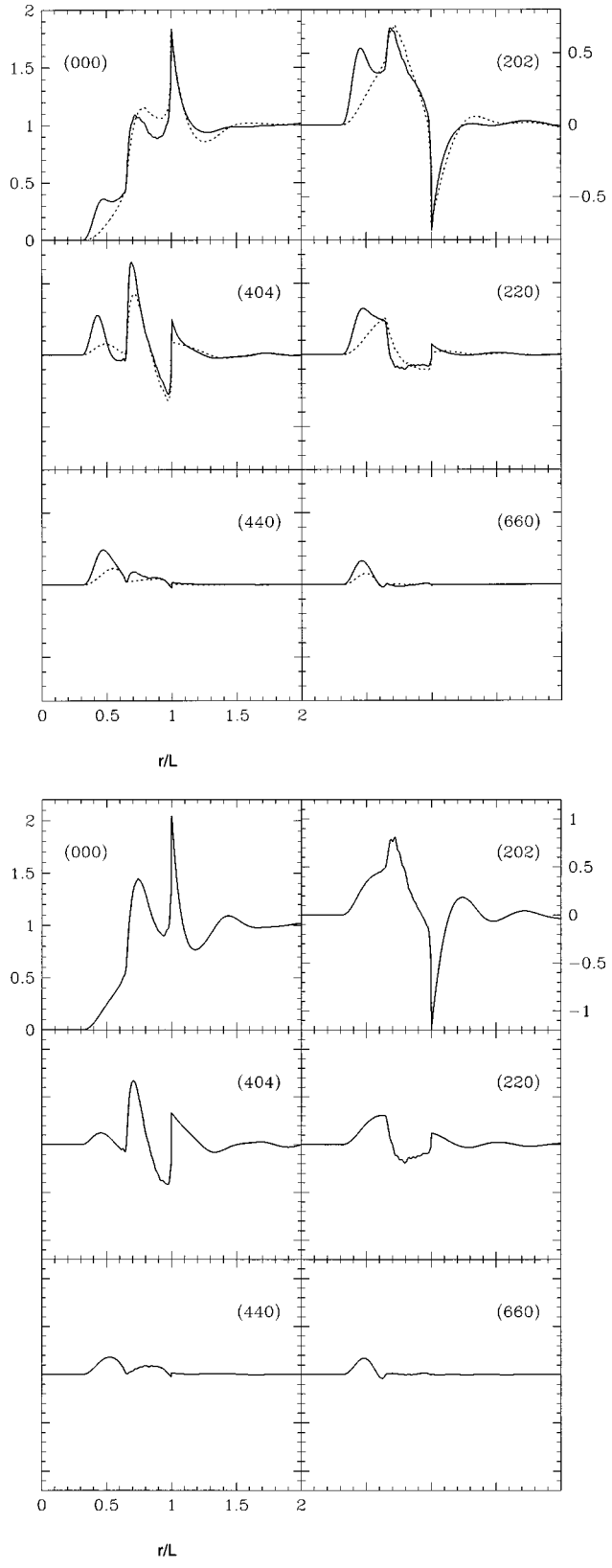

FIG. 3. (a) The pair distribution function expansion coefficients $g^{mnl}(r)$ for cut sphere thickness $L^*=0.3$ and for density $\rho^*=1.7037$. Solid line is for HNC and dotted one for PY. The vertical labeling of the upper right panel is for all (mnl) different from 0. (b) Same as in (a) but for density $\rho^*=2.222$. Only PY results are plotted in solid lines.

simulation results. This will be clear in the next section. In Fig. 3(b) we have plotted the results of the PY theory at the highest density it could be solved. We see that globally the same tendencies observed at the lower density are again reproduced with more structure. In particular the first peaks in $g^{000}(r)$ moves toward $r^*\simeq 0.7$ which is approximatively the perpendicular packing. No stack piling is observed. So the PY theory does not predict a cubatic ordered phase, not even a metastable one.

We turn now to the case $L^*=0.2$ for which a stable cubatic order is observed in the simulations. In Fig. 4(a) we have plotted the $g^{mnl}(r)$ for HNC and PY at the maximum density at which HNC could be solved $\rho^*=2.125$. The global features are quite similar to that observed in Fig. 3(a), except for the positions and the magnitude of the peaks. Again HNC shows a tendency to a three particles short stack. It is difficult to conclude a tendency toward cubatic long range ordering because of the lack of structure beyond $r^*=1$ for $g^{440}(r)$. The only evidence comes from the higher position of the second peak in $g^{000}(r)$ (which we recall indicates rather a perpendicular alignment), and the somewhat longer range of the function $g^{440}(r)$ which develops a small positive tail at large r and is no longer oscillatory. However, this trend is not as spectacular as that observed in the nematic type alignment for prolate particles.[5] The reason might be that cubatic ordering involves at least three particle correlations and these might not be well described at the level of HNC, especially in the long range part. The PY theory has grossly the same features as in Fig. 3(a). In Fig. 4(b) we plotted the PY results at a higher density, in fact the smallest density for which computer simulation results are also reported $\rho^*=2.963\,75$ (which corresponds to $\rho^*=0.51$ in the units of Ref. 4). Indeed, all correlation functions reported in Ref. 4 are for densities either very close to the transition region or in the ordered phase, both cases being unreachable from PY and HNC. In this lucky case we see that the PY theory definitely is out of focus as compared with the simulations. This is strikingly clear for $g^{000}(r)$, for which in particular the first peak seen in HNC is also reproduced by the simulations, the second peak being smaller that the PY first peak, a feature again shared by the HNC theory. One can infer that HNC and computer simulation results of the $g^{mnl}(r)$ are in quite good agreement for the whole density solution range of the HNC theory. PY predicts more structure for $r^*>1$ than the simulation results. For $g^{220}(r)$ PY completely misses the first large peak observed in the simulations which is the onset of a first neighbor piling. However, it describes quite well the secondary structure near $r^*=0.5$. For $g^{440}(r)$, however, the simulations clearly show a large first peak and a long range tail, totally absent from PY. On the other hand, the first peak of PY is much larger than for simulations, indicating again that perpendicular alignment is the major feature of PY theory, entirely overriding the short range columnar packing. These features, entirely missing from the PY theory, are the major arguments put forward in Ref. 4 to support the cubatic ordering. We conclude that PY has no tendency toward cubatic order.

Finally the case $L^*=0.1$ is shown in Fig. 5, again at the highest density for which HNC could be solved. We note

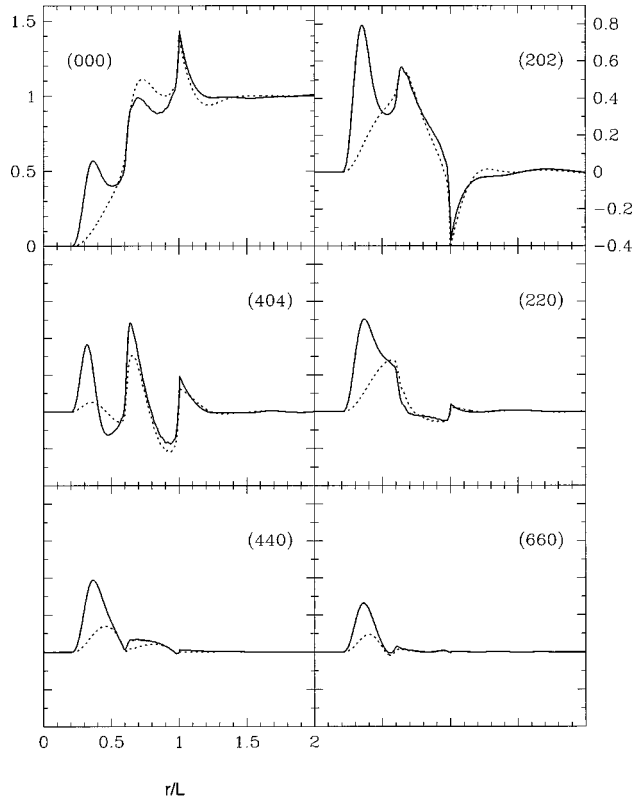

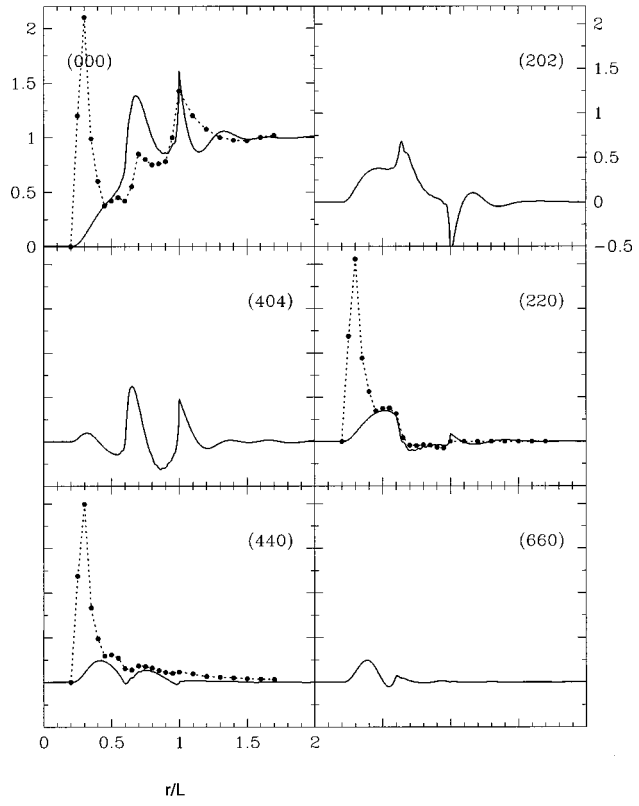

FIG. 4. (a) Same as in Fig. 3(a) but for cut sphere thickness $L^*=0.2$ and density $\rho^*=2.125$. (b) Same as in Fig. 4(a) but for density $\rho^*=2.963\,75$. Only PY results are plotted in solid lines together with simulation results from Ref. 4 plotted in dots.

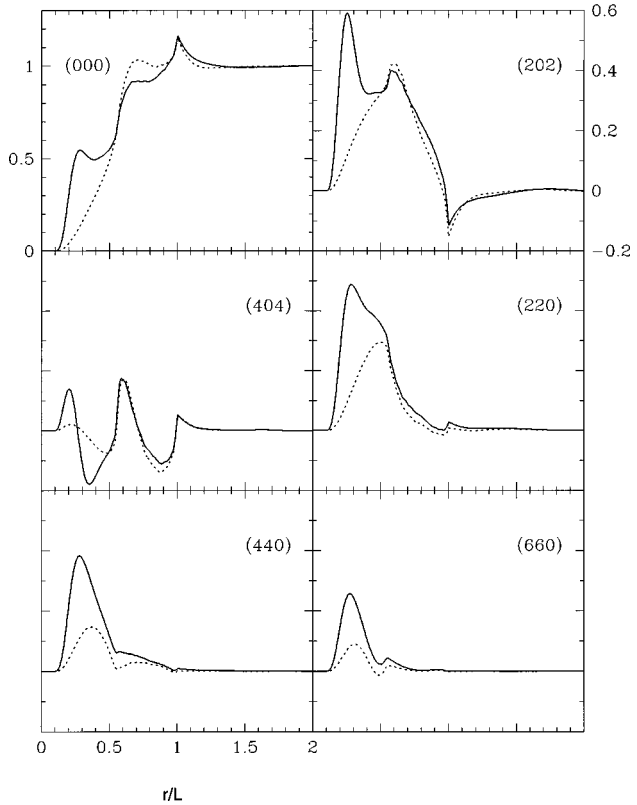

FIG. 5. Same as in Fig. 3(a) but for cut sphere thickness $L^*=0.1$ and density $\rho^*=2.5$.

here that HNC has somewhat broader first and second peaks (indicating a more than three particle short range structure), and $g^{220}(r)$ now shows a distinct long range feature, which was absent from the previous cases, and is indicative of a tendency toward nematic ordering. PY theory is inconclusive, even at higher densities.

We note that the somewhat better agreement observed between the HNC compressibility pressures and the computer simulations for the more oblate shapes tends to indicate that $c^{000}(r)$, and thus $g^{000}(r)$, might be accurately obtained from HNC. This is compatible with that observed for prolate shapes.[5,21] This could be checked for the cut sphere case if computer simulations of the $g^{mm0}(r)$ were available for densities in the isotropic phase.

Finally the direct correlation function for the geometrical approach is compared in Fig. 6 with that from PY and HNC for $L^*=0.2$ and $\rho^*=1.75$. As noted in Ref. 12 we observe that the agreement is not so great. This situation is better for $L^*=0.3$, but it is worse with more oblate shape $L^*=0.1$. In all cases, there is a better agreement in the low density region. The deterioration of the quality of the geometrical theory at high densities indicates that the density coupling that builds up in the structure for PY and HNC theories is not so well described by the geometrical approach. We suspect that the difference with prolate shapes, for which the agreement is very good even at high elongations, comes from the incapacity of the geometrical approach to describe short columnar type ordering which appears even in the isotropic phase of oblate shaped particles. This situation involves correlations higher than two bodies, a feature which is not in-

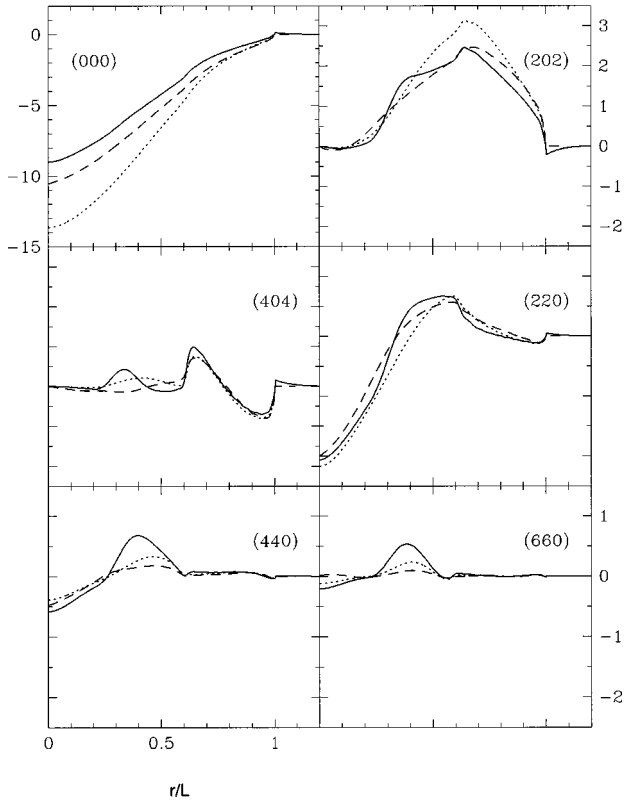

FIG. 6. The expansion coefficients of the DCF $c^{mnl}(r)$ for cut sphere of thickness $L^*=0.2$ at density $\rho^*=1.75$. The solid line is for HNC, the dotted one for PY, and the dashed one for the geometrical DCF. The vertical labeling convention are as in Fig. 1.

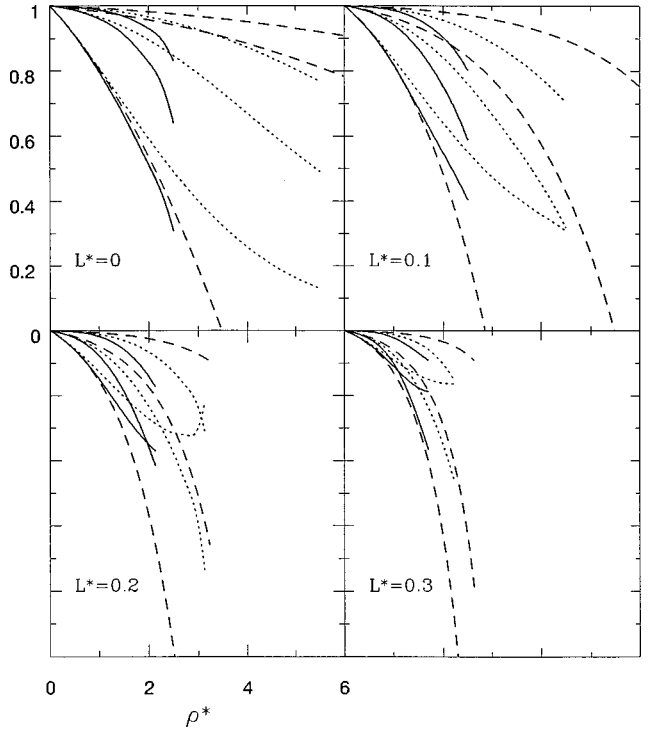

FIG. 7. The Δ_m ($m=2$, 4, 6) for cut spheres of thicknesses $L^*=0$, 0.1, 0.2, and 0.3. The solid line is for HNC, the dotted one for PY, and the dashed one for the geometrical DCF.

corporated in Eq. (8). A similar argument can also explain that the prediction of cubatic order by the same theory occurs for thicknesses around and above $L^*=0.5$, values that are much higher than the correct ones. This point is discussed below.

C. Prediction of ordered phases: The instability criteria

The instability of the isotropic phase occurs when one of the mode Δ_m goes to zero:[5]

$$\Delta_m=1-\rho\tilde{c}^{mm0}(k=0)/\sqrt{(2m+1)}. \tag{14}$$

For nematic type instabilities, Δ_2 decreases to zero faster than the other modes. In fact, Δ_2 is exactly the reduced inverse Kerr constant[5] which is known to diverge at the limit of stability of the isotropic phase. This is linked to the appearance of long range orientational density fluctuations which finally tend to destabilize the isotropic phase. Using the OZ equation, it is easy to show[5] that one also has $\Delta_m=1/(1+\rho\tilde{h}^{mm0}(k=0)/\sqrt{(2m+1)})$ where $h(1,2)=g(1,2)-1$ is the pair correlation function. At the limits of the isotropic-cubatic phase it is $h^{440}(r)$ that is long ranged,[4] thus one expects naturally Δ_4 to vanish near this limit. It is important to note that even if an instability is predicted, it does not necessarily mean that there is a phase transition. The latter can be confirmed only if the free energies of the two phases can be calculated. In the present case the free energy of the ordered phase is totally unknown for either of the theories discussed here. Consequently, only a guess of the ordered phase can be formulated in our context.

The integral equations, in practice, cannot be solved for all densities until the limit $\Delta_m=0$ is reached. The solution is lost at a somewhat lower density and one can extrapolate the curves to zero in order to find the predicted instability density. The situation is similar to that observed in other systems (liquid–gas or Coulombic) solved by such theories and, despite minute numerical care, the solution is always lost at some density.[22,23] This seems a mathematical feature of the integral equations. As the critical region is approached it seems that a better description of the fluctuations is needed, meaning that higher order graphs must be included in order to properly describe the short and long range correlations. No simple procedure to overcome this insufficiency has been found yet. The geometrical approach is free from this constraint and this is a quite attractive feature. The instability criteria for the geometrical DCF can be derived from Eqs. (8)–(10). One obtains

$$\Delta_m=1-\rho\chi_0\frac{\tilde{F}_M^{mm0}(k=0)}{\sqrt{(2m+1)}}. \tag{15}$$

From this equation it is clear that if $\tilde{F}_M^{440}(0)>\tilde{F}_M^{220}(0)$, one will have a destabilization of the isotropic phase toward a cubatic ordering. In view of the results of Table I, it is thus clear that for thicknesses greater that $L^*=0.5$ the geometrical approach predicts the possibility of the cubatic long range ordering. This is clearly in variance with the computer simulation results.

In Fig. 7 we have plotted the Δ_m ($m=2$, 4, 6) for PY and HNC theories as well as for the geometrical approach, and

for the thicknesses of $L^*=0$, 0.1, 0.2 and 0.3. For thicknesses 0 and 0.1, HNC and the geometrical theory show that Δ_2 decreases faster than the other two modes. This indicates a clear tendency toward nematic ordering, in agreement with the computer simulations results. The HNC results for the structure also support this conclusion. The instability density is found by extrapolating Δ_2 to zero, which is not difficult to achieve. We note that the geometrical approach predicts instabilities relatively close to that of HNC, a feature already observed in Ref. 12. The PY theory shows a different behavior, as Δ_2 has lower values than the other modes but has a slower decrease. This makes difficult the precise extrapolation of Δ_2. The situation is different for less oblate shapes for which Δ_2 stops at values too high to permit a proper extrapolation. If we do so, we get values of densities too high when compared to those for HNC or the geometrical approach. The reason why the PY values stop too high is that the PY theory does not develop long range orientational correlations before the numerical solution is lost. These conclusions are identical to those reached in earlier works.[5]

For the thickness $L^*=0.2$ both integral equations show a new feature. The curves Δ_2 and Δ_4 cross over, indicating that the cubatic type long range correlations grow faster that the nematic ones. We note that while HNC solution stops at quite high values for Δ_4 the corresponding PY values go almost to zero. However, for the PY case, this does not prove that long range fluctuations are growing. A careful analysis of $g^{440}(r)$ shows that the growth of the first peak just before $r^*=1$ is the major responsible for the increase of the integrand in the definition for Δ_4. Thus as noted in the previous section, it is the growth of the two particles perpendicular ordering which is responsible for the dramatic decrease of Δ_4 for PY. This situation is somewhat similar to that observed for two or three tangent hard spheres chains[16] in which case it was found that Δ_4 decreased faster than Δ_2, although not to values as low as those observed in the present case. Moreover we note that Δ_2 for the PY theory increases quite vigorously at high densities, indicating that the parallel ordering is lost, which is consistent with the bad description of the piling effect by the same theory. In view of these argument, it is difficult to conclude that the PY theory is able to predict a cubatic ordering, mainly when the short range piling is completely missing. The HNC results for Δ_4 are not too low and it is hard to obtain a accurate value for the extrapolated density. The geometrical approach on the other hand, predicts incorrectly a nematic type ordering.

Finally for the thickness $L^*=0.3$ both integral equation theories have values of Δ_4 and Δ_2 that cross over, again indicating a possibility of cubatic ordering. But the last values obtained for Δ_4 are too high to permit an accurate extrapolation to zero. One could say that this case is inconclusive, at least in the case of the HNC theory. The PY theory definitively has no cubatic ordering tendencies, for reasons mentioned in the previous section.

In order to clearly sort out the situation for the HNC theory, we have solved this equation for several intermediate thicknesses. We found that an empirical criteria for cubatic ordering is obtained when both the following criteria are achieved. First, the long range part of $g^{440}(r)$ must be positive and nonoscillatory. A consequence of this is that Δ_4 will be at least smaller than 0.6 at the highest density for which the integral equation can be solved. So the second criteria is that Δ_4 must be smaller than 0.6. But in some circumstances this second criteria was achieved when the first one was not. For thicknesses larger than $L^*=0.24$ we found that Δ_4 was reaching limiting values below 0.6 but had a tendency to curve outward, like the PY results for Δ_2 for thicknesses $L^*=0$ and 0.1. It is clearly impossible in such a case to extrapolate to zero in a reasonable density range. This was consistent with the fact that the long range part of $g^{440}(r)$ was oscillatory with small negative values in some parts. Between thicknesses $L^*=0.12$ and $L^*=0.18$, the Δ_4 term had the correct convexity, but values lower that 0.6 could not be reached (like in the case of $L^*=0.3$). Using the two empirical rules, one can plot the tentative phase diagram, or rather an instability diagram for the HNC cut sphere fluids. This is sketched in Fig. 8 where we have plotted our extrapolated guess of the HNC instability lines on the phase diagram obtained by Veerman and Frenkel.[4] We see that the HNC theory is in reasonable agreement for the nematic-isotropic branch, but not so good for the cubatic region. In all cases HNC predicts an instability at densities *lower* than the computer simulation results. Finally we note that the geometrical approach is relatively close to the HNC line for the isotropic-nematic branch, but for somewhat lower densities (see Fig. 7). Between $L^*=0.12$ and $L^*=0.18$ nothing in the behavior of HNC seems to indicate a possible instability toward the columnar phase predicted by the computer simulations. We note that the isotropic-columnar transition is strongly first

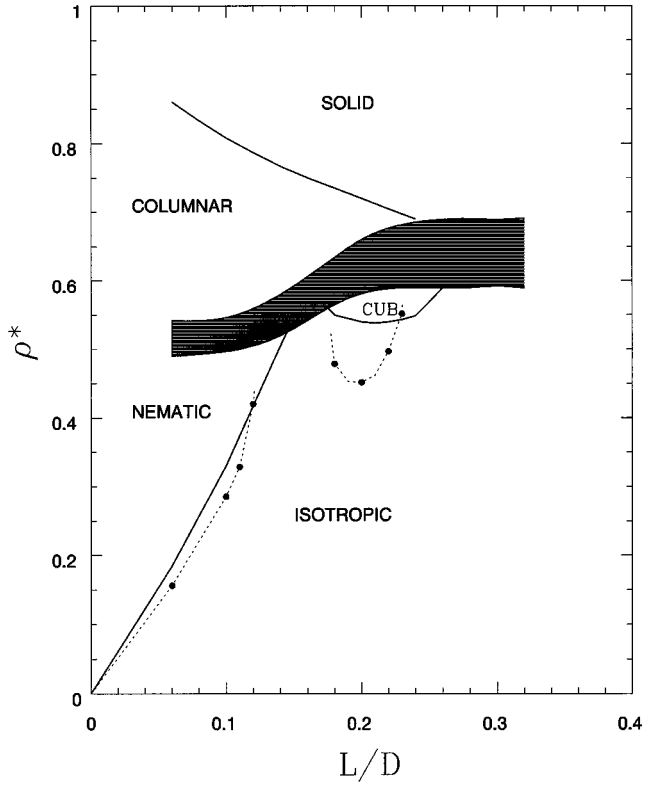

FIG. 8. The phase diagram of the cut spheres sketched from Ref. 4. The HNC instability lines are plotted in dots (see text).

order. Hence we think that HNC behaves here as for the hards sphere case, for which it does not predict any instability toward the solid phase.

The case $L^*=0$ (platelet fluid) is particularly interesting. The simulations indicate that the isotropic-nematic transition takes place for $\rho^*\sim 4.04$. We see that the geometrical approach predicts an IN instability at a somewhat lower density $\rho^*\sim 3.5$. The HNC results also indicate an IN instability for a lower density $\rho^*\sim 3$ whereas the PY theory is quite inconclusive. These results are strikingly similar to those obtained for the 2D hard needles fluid[24] which represents a limiting case of the hard ellipse fluid in the same way the platelet fluid is a limiting case of the cut sphere fluid.

IV. CONCLUSION

In the present work, the PY and HNC integral equations are solved for hard cut sphere fluids of various thicknesses. We are particularly interested to see if they correctly describe the onset of nematic ordering for thicknesses lower than 0.12 as well as the cubatic ordering for cut sphere thicknesses ranging from 0.18 to 0.24. After proper analysis only the HNC theory is shown to adequately describe both ordering. Even though the PY results may seem to indicate a cubatic ordering, analysis of the structure prevents reaching positive conclusions. The same theory is equally unable to predict nematic ordering, in accord with previous calculations.[5]

The geometrical approach for the DCF that was proposed recently,[12] despite some success in rendering the gross features of the DCF, predicts the possibility of a cubatic phase for thicknesses too large. On the other hand, the same approach predicts a nematic phase in the correct range of densities and thicknesses. The reason for this failure might be attributed to the fact that the definition of the geometrical DCF in Eq. (8) does not account for more than pair correlations. Indeed, in the premises of cubatic ordering at least three particles correlations must be described properly. We note that the information about the cubatic ordering is already contained in the Mayer function [as the analysis of the $F_M^{mm0}(k=0)$ reveals], which means that a pair level description is sufficient. This analysis shows in particular that cubatic phases can be predicted for thicknesses larger than $L^*=0.5$. But it is the density couplings that will bring out the effects of more than three particle correlations, thus shifting the isotropic-cubatic transition toward lower thicknesses. These effects are not contained in the geometrical DCF, but to some extent in the integral equations.

The HNC theory, on the contrary, describes quite well the three particles short range correlations but this effect is weaker in the long range part. This is in contrast with the good results obtained by the same theory when describing nematic pretransitional ordering. Clearly, the HNC theory incorporates a better global description of the pair correlations than it does for the triplet or higher order ones. We note, however, that the HNC theory does hint of an instability toward the cubatic phase, in which case it does have a positive nonoscillatory long range tail in $g^{440}(r)$. We find here that the detailed analysis of the cut sphere fluid might help in shedding some light on the diagrammatic nature of the two integral equations that are mostly used, particularly in what concerns the higher order correlations that are embodied in these approximations. A systematic study, including the so-called bridge diagram, at least for the first few terms is feasible although being quite involved. We do not think that artificial procedures mixing the PY and HNC equations might help solve this problem, mainly because both integral equations apparently do not handle more than two body correlations in an entirely satisfactory manner. In view of these results, one might wonder how good would an extension of either theories in an ordered phase be (nematic or other), as obviously in such a case higher order correlations are crucially important. Further work in these directions must explicitly account in a proper way for the three or more particle correlation in an approximate expression for higher order graphs in the PY, or better in the HNC theory.

[1] S. Chandrasekhar, *Liquid Crystals* (Cambridge, 1992).
[2] P. Bolhuis and D. Frenkel, J. Chem. Phys. **106**, 666 (1997).
[3] D. Frenkel, in *Liquids, Freezing and Glass Transition* (Elsevier, New York, 1991).
[4] J. A. C. Veerman and D. Frenkel, Phys. Rev. A **41**, 3237 (1990).
[5] A. Perera, P. G. Kusalik, and G. N. Patey, J. Chem. Phys. **87**, 1295 (1987).
[6] H. Azzouz, J. M. Caillol, D. Levesque, and J. J. Weis, J. Chem. Phys. **96**, 4551 (1992).
[7] L. Blum and A. J. Torruella, J. Chem. Phys. **56**, 303 (1972).
[8] F. Lado, Mol. Phys. **47**, 283 (1982).
[9] P. H. Fries and G. N. Patey, J. Chem. Phys. **82**, 429 (1985).
[10] P. G. Ferreira, A. Perera, M. Moreau, and M. M. Telo da Gama, J. Chem. Phys. **95**, 7591 (1991).
[11] A. Chamoux, Thèse de Doctorat de l'Université Pierre et Marie Curie, 1997.
[12] A. Chamoux and A. Perera, J. Chem. Phys. **104**, 1493 (1996).
[13] H. Reiss, H. L. Frisch, and J. L. Lebowitz, J. Chem. Phys. **31**, 369 (1959).
[14] Y. Rosenfeld, Phys. Rev. Lett. **63**, 3387 (1989).
[15] E. Kierlik and M. L. Rosinberg, Phys. Rev. A **42**, 3382 (1990).
[16] A. Chamoux and A. Perera, Mol. Phys. **93**, 649 (1998).
[17] A. Perera and A. Chamoux, unpublished results.
[18] L. Onsager, Ann. (N.Y.) Acad. Sci. **51**, 627 (1949).
[19] P. G. de Gennes, *The Physics of Liquid Crystals* (Clarendon, Oxford, 1974).
[20] R. Eppenga and D. Frenkel, Mol. Phys. **52**, 1303 (1984).
[21] A. Perera, and G. N. Patey, J. Chem. Phys. **89**, 5861 (1988).
[22] L. Belloni, J. Chem. Phys. **98**, 8080 (1993).
[23] P. G. Ferreira, R. L. Carvalho, M. M. Telo da Gama, and A. G. Schlijper, J. Chem. Phys. **101**, 594 (1993).
[24] A. Chamoux, A. Perera, and P. G. Ferreira (in preparation).